water

Article

# Optimal Flood-Control Operation of Cascade Reservoirs Using an Improved Particle Swarm Optimization Algorithm

**Yanfang Diao [1], Haoran Ma [2], Hao Wang [1], Junnuo Wang [3], Shuxian Li [1], Xinyu Li [1], Jieyu Pan [4] and Qingtai Qiu [1,5,*]**

[1] College of Water Conservancy and Civil Engineering, Shandong Agricultural University, Tai'an 271018, China; diaoyanfang@sdau.edu.cn (Y.D.); wh17861509336@163.com (H.W.); lsxian2000@163.com (S.L.); lxy330613@163.com (X.L.)
[2] School of Hydraulic Engineering, Dalian University of Technology, Dalian 116024, China; mahaoran0814@163.com
[3] Shui Fa Planning & Design Co., Ltd., Jinan 250000, China; owenzqq@126.com
[4] School of Earth Sciences and Engineering, Nanjing University, Nanjing 210023, China; panjy_0827@163.com
[5] State Key Laboratory of Simulation and Regulation of Water Cycle in River Basin, China Institute of Water Resources and Hydropower Research, Beijing 100038, China
* Correspondence: qqt31415926@163.com

**Abstract:** Optimal reservoir operation is an important measure for ensuring flood-control safety and reducing disaster losses. The standard particle swarm optimization (PSO) algorithm can find the optimal solution of the problem by updating its position and speed, but it is easy to fall into a local optimum. In order to prevent the problem of precocious convergence, a novel simulated annealing particle swarm optimization (SAPSO) algorithm was proposed in this study, in which the Boltzmann equation from the simulated annealing algorithm was incorporated into the iterative process of the PSO algorithm. Within the maximum flood peak reduction criterion, the SAPSO algorithm was used into two floods in the Tianzhuang–Bashan cascade reservoir system. The results shown that: (1) There are lower maximum outflows. The maximum outflows of Tianzhuang reservoir using SAPSO algorithm decreased by 9.3% and 8.6%, respectively, compared with the measured values, and those of Bashan reservoir decreased by 18.5% and 13.5%, respectively; (2) there are also lower maximum water levels. The maximum water levels of Tianzhuang reservoir were 0.39 m and 0.45 m lower than the measured values, respectively, and those of Bashan reservoir were 0.06 m and 0.46 m lower, respectively; and (3) from the convergence processes, the SAPSO algorithm reduced the convergence speed in the early stage of convergence and provided a superior objective function value than PSO algorithm. At the same time, by comparing with GA algorithm, the performance and applicability of SAPSO algorithm in flood operation are discussed further. Thus, the optimal operation model and SAPSO algorithm proposed in this study provide a new approach to realizing the optimal flood-control operation of cascade reservoir systems.

**Keywords:** cascade reservoirs; optimal operation; SAPSO algorithm; outflow

check for updates

**Citation:** Diao, Y.; Ma, H.; Wang, H.; Wang, J.; Li, S.; Li, X.; Pan, J.; Qiu, Q. Optimal Flood-Control Operation of Cascade Reservoirs Using an Improved Particle Swarm Optimization Algorithm. *Water* **2022**, *14*, 1239. https://doi.org/10.3390/w14081239

Academic Editor: Guido Paliaga

Received: 11 March 2022
Accepted: 9 April 2022
Published: 12 April 2022

**Publisher's Note:** MDPI stays neutral with regard to jurisdictional claims in published maps and institutional affiliations.

**Copyright:** © 2022 by the authors. Licensee MDPI, Basel, Switzerland. This article is an open access article distributed under the terms and conditions of the Creative Commons Attribution (CC BY) license (https://creativecommons.org/licenses/by/4.0/).

## 1. Introduction

Floods are among the most frequent natural disasters worldwide. According to the 2020 Global Natural Disaster Assessment Report [1], 313 natural disasters (excluding epidemic diseases) occurred in 2020, of which 193 (or 61.66%) were floods. Furthermore, floods caused 6171 deaths in 2020 (accounting for 41% of all deaths caused by disasters), affected 33.22 million people (accounting for 34% of all natural disaster victims), and caused direct economic losses of USD 51.5 billion. Reservoirs have therefore been constructed to serve as important water-conservancy projects that provide flood control and disaster risk reduction while also playing important roles in water supply, irrigation, navigation, and aquaculture. Scientific and reasonable reservoir operation schemes can ensure the effective use of reservoirs in these roles. Because the optimal operation strategy is more effective than the conventional operation strategy in ensuring the safety of the reservoir upstream and downstream and reducing flood losses, various optimization algorithms have been used to optimize flood-control operations since the 1960s.

Current optimization methods employ either conventional optimization algorithms or heuristic intelligent optimization algorithms. Conventional optimization algorithms include linear programming (LP), nonlinear programming (NLP), dynamic programs (DP) [2], and the progressive optimality algorithm (POA) [3] as well as associated improved algorithms. For instance, Manne [4], Niu et al. [5], Su et al. [6], and Dogan et al. [7] applied the LP, mix-max LP, mixed-integer LP, and hybrid LP and NLP, respectively to determine the optimal reservoirs or hydropower reservoirs discharges. Young [8] first applied DP to solve a single-reservoir operation problem, and then the multi-stage DP, stochastic DP, coupling parallel DP with importance sampling and successive approximation, hybrid DP and LP, and spark-based parallel DP models were put forward by Ji et al. [9], Wu et al. [10], He et al. [10], Zhong et al. [11], and Ma et al. [12], respectively. Because POA can alleviate the problem of "curse of dimensionality", Zhong et al. [13], Jiang et al. [14], Zhou et al. [15], Chen et al. [16], and Ji et al. [17] proposed the orthogonal POA, multi-stage POA, DP combined with POA, enhanced POA and DP hybrid approach, and nested POA to solve the optimal operation strategy. However, when faced with a complex flood-control system composed of reservoir groups, flood storage and detention areas, lakes, and other flood-control projects, conventional optimization algorithms exhibit obvious limitations, such as low convergence efficiency and dimensionality. Advances in modern computing technology have led to the development of heuristic intelligent algorithms employing the principles of biology, physics, and artificial intelligence that can address such limitations, including the genetic algorithm (GA) [18,19], non-dominated sorting genetic algorithm (NSGA-II) [20,21], artificial neural network (ANN) [22,23], particle swarm optimization (PSO) [12,24], ant colony algorithm [25,26], simulated annealing (SA) [27,28], immune algorithm [29], evolutionary algorithm [30,31], cultured evolutionary algorithm [32], and fruit fly optimization algorithm [33], all of which represent general-purpose stochastic search methods that simulate natural selection and biological evolution [34]. Because they can be directly applied to complex problems with nonlinear, discontinuous, non-differentiable, and multi-dimensional characteristics, they have been widely used to optimize reservoir operation.

Among the above heuristic intelligent algorithms, the PSO algorithm and its variants has been widely used in solving water resources optimization problem because of its simple structure, limited number of parameters, and light calculation requirements [35]. For example, in the prediction of hydrological elements, Chau [36] applied PSO algorithm to real-time water level prediction in a river; Ghorbani et al. [37] proposed quantum-behaved PSO coupled with ANN to predict daily evaporation rate; Niu et al. [38] combined quantum-behaved PSO with extreme learning machine to predict the daily runoff of the Xinfengjiang reservoir in China. In the optimization of model parameters, Afshar et al. [39] applied multi-objective PSO for optimal calibration of water quality model; Kisi et al. [40] applied PSO-ANN to model groundwater parameters; Ehteram et al. [41] applied coupled bat algorithm with PSO to optimize the parameters of a Muskingum model for accurate flood routing in three different case studies in the USA and UK. In the water-distribution network design, Ezzeldin et al. [42] and Sedki et al. [43] applied PSO and hybrid PSO and differential evolution algorithms to minimize total design cost of water-distribution networks, respectively. PSO algorithm is the most widely used in reservoir operation; for example, Kumar et al. [44] applied PSO to derive operating policies for a multi-purpose reservoir system; Hojati et al. [45] applied and compared the applications of multi-objective PSO and NSGA-II to obtain optimal operation of two reservoirs for the objectives of maximizing income from power production and flood control; Guo et al. [46] combined the multi-population mechanism with non-dominated sorting PSO for minimization of pump station costs and maximization of the lowest water level at Guanyinge reservoir; Zhong et al. [47] applied chaotic PSO to obtain maximum power generation of a cascade reservoir in the Upper Yellow River, China; Yaseen et al. [48] applied hybrid bat algorithm-PSO to optimize power production and irrigation supply of a multi-purpose reservoir system in the state of Karnataka, India; Trivedi et al. [49] put forward a time-variant elitist mutation multi-objective PSO to derivation and performance evaluation of optimal operating policies for a reservoir; Ma et al. [12] proposed the spark-based parallel PSO method via cloud computing for the cascade eight-reservoir system in the Yuanshui basin in China; and Mahdi et al. [50] proposed and evaluated an integrated framework to optimize reservoir operation using PSO in which hydropower loss and economic loss of irrigation supply were minimized, while ecological degradations at downstream river were alleviated.

However, while the PSO algorithm is widely used, it has proven easy for it to fall into a locally optimal solution, which makes the optimal solution worse than other algorithms in some cases. In contrast, the SA algorithm accepts the new state with a specified probability; that is, even if there are multiple local optimal solutions to a problem, it can effectively prevent the result from falling into a local extreme point. In this manner, the SA algorithm can compensate for the shortcomings of the PSO algorithm. In this study, a simulated annealing particle swarm optimization (SAPSO) algorithm was therefore proposed to realize optimal flood-control operation of cascade reservoir systems by introducing the Boltzmann equation from the SA algorithm into the iterative process of the PSO algorithm, effectively addressing the tendency of the latter to fall into a locally optimal solution.

The remainder of this study is organized as follows: Section 2.1 describes the optimal cascade reservoir flood-control operation model; Section 2.2 presents the PSO algorithm, SA algorithm, SAPSO algorithm, and procedure for determining the optimal cascade reservoir operation scheme using the proposed SAPSO algorithm; Section 3 introduces the study area, data processing, and parameter setting; Section 4 illuminate and discusses the results of a case study application of the proposed SAPSO algorithm; and Section 5 provides a summary of the conclusions.

## 2. Methods

The development of the optimal reservoir flood-control operation strategies can be generally described in the following two-step process: (1) Choose an optimization criterion to develop a corresponding objective function, then establish an optimal flood-control operation model for the given input data and constraints [51]. (2) Use optimization algorithms to solve the model and obtain the optimal reservoir operation scheme [52]. Thus, this section consists of the construction of the optimal cascade reservoir flood-control operation model and the solution of this model using SAPSO algorithm.

### 2.1. Optimal Cascade Reservoir Flood-Control Operation Model

The objective function and constraints for the proposed optimization model are described in this section. The meanings and units of parameters and variables in this section are listed in Table 1.

**Table 1.** Meanings and units of the parameters and variables.

| Parameters or Variables | Meanings | Units |
|---|---|---|
| $M$ | The number of reservoirs in the cascade reservoir system | - |
| $T$ | Number of operation periods | - |
| $q_{\mathrm{i}}(t)$ | Outflow of reservoir $i$ at time $t$ | $\mathrm{m}^3/\mathrm{s}$ |
| $R_{i+1}(t)$ | Inflow between reservoirs $i$ and $i+1$ | $\mathrm{m}^3/\mathrm{s}$ |
| $Q_i(t)$ | Inflow to reservoir $i$ at time $t$ | $\mathrm{m}^3/\mathrm{s}$ |
| $V_i(t)$ | Storage capacity of reservoir $i$ at time $t$ | $\mathrm{m}^3$ |
| $t'$ | Time when the outflow from reservoir $i$ arrives at reservoir $i+1$ | h |
| $V_i(t)_{\max}$ | Upper bound of the storage capacity of reservoir $i$ at time $t$ | $\mathrm{m}^3$ |
| $V_i(t)_{\min}$ | Lower bound of the storage capacity of reservoir $i$ at time $t$ | $\mathrm{m}^3$ |
| $q_i\,[V_i(t)]$ | Maximum outflow capacity of reservoir $i$ when the storage capacity is $V_i(t)$ | $\mathrm{m}^3/\mathrm{s}$ |

#### 2.1.1. Objective Function

There are three main flood-control optimization criteria for reservoirs [53]: (1) maximum reduction in flood peak, (2) minimum flood duration, and (3) minimum flood loss or flood-control cost. The maximum reduction in the flood peak was defined in this study as the objective function to determine the optimal outflows of a cascade reservoir system.

The objective of the maximum reduction in the flood peak criterion is to reduce the flood peak to the extent possible to ensure the flood-control safety of the dam or reservoir area. A general form of this objective function in the case of a cascade reservoir system can be written as [54]

$$\min fun = \min \sum_{i=1}^{M} \sum_{t=1}^{T} (q_i(t) + R_{i+1}(t))^2 \tag{1}$$

#### 2.1.2. Constraints

This study identified four constraints on the proposed cascade reservoir flood-control operation model: the water balance, hydraulic connection, storage capacity, and outflow. All variables in all constraints were positive only.

(1) The water balance constraint is given by

$$(Q_i(t) - q_i(t))\Delta t = V_i(t) - V_i(t-1) \tag{2}$$

(2) The hydraulic connection constraint is given by

$$Q_{i+1}(t) = q_i(t - t') + R_{i+1}(t) \tag{3}$$

(3) The storage capacity constraint is defined as

$$V_i(t)_{\min} \le V_i(t) \le V_i(t)_{\max} \tag{4}$$

(4) The outflow constraint is given by

$$q_i(t) \le q_i[V_i(t)] \tag{5}$$

### *2.2. Optimal Operation of Cascade Reservoir System Using SAPSO Algorithm*

#### 2.2.1. PSO Algorithm

The PSO algorithm is an intelligent scheme categorized as a metaheuristic optimization algorithm. It was first proposed in 1995 by Dr. James Kennedy, an American social psychologist, and Dr. Russell Ebethart, an electrical engineer, who were inspired by artificial life and evolutionary computation theory [55]. The PSO algorithm was developed based on the paradigm of swarm intelligence as inspired by the social behavior of animals such as fish and birds when seeking food. The PSO algorithm was first designed to solve nonlinear continuous optimization problems and has been widely used in job scheduling, decision making, pattern recognition, real-time robot path design, and other applications because of its numerous advantages. These advantages include structural simplicity, easy implementation, the need for fewer parameters that must be tuned, and low computational requirements that allow the algorithm to be implemented on a low-cost processor platform.

A swarm in PSO consists of a set of particles that represent a population of candidate solutions. Any particle has a specific position in a search space composed of all possible solutions to the problem. The PSO algorithm attempts to find the best particle from among all possible solutions in this space. The first step is to initialize *sizepop* particles randomly in the *dim*-dimensional search space, each of which has associated attributes, such as fitness (calculated using the objective function), position, and velocity. The fitness of a particle describes the distance from the position of the particle to the global optimal solution. When solving the maximization problem, the greater the fitness value of a particle, the better the solution it provides, whereas the opposite is true for the minimization problem. Each particle changes its position after each iteration based on the velocity updates. This change is influenced by two "best" values: the one known as "Pbest" or personal best describes the best solution achieved by a given particle and the other, known as "Gbest" or global best, describes the best solution achieved by any particle among the entire set of particles in the solution space. The velocity and position of each particle were used to reposition the particle using the following equations:

$$v_{jh}^{k+1} = wv_{jh}^{k} + c_1 rand_1 \left( Pbest_{jh}^{k} - x_{jh}^{k} \right) + c_2 rand_2 \left( Gbest_h - x_{jh}^{k} \right) \tag{6}$$

$$x_{jh}^{k+1} = x_{jh}^{k} + v_{jh}^{k+1} \tag{7}$$

where ${x_{jh}}^k$ and ${v_{jh}}^k$ describe the position and velocity of the $j$th particle in the $h$th spatial dimension at iteration $k$; $w$ is the inertial weight; $c_1$ and $c_2$ are learning factors, which are non-negative constants; $rand_1$ and $rand_2$ are two independent random numbers taken in the range of (0, 1); ${Pbest_{jh}}^k$ is the personal best position of the $j$th particle in the $h$th spatial dimension at iteration $k$; and $Gbest_h$ is the global best position in the $h$th spatial dimension in each iteration among the entire set of particles.

When the positions of all particles have been updated, the algorithm determines whether the Pbest and Gbest values have changed; if so, it continues to search for new positions through continuous iteration following the above method until the maximum number of iterations is reached, or the searched optimal solution satisfies the requirements.

### 2.2.2. SA Algorithm

The SA algorithm is a probabilistic optimization method introduced by Kirkpatrick et al. [56] and inspired by the physical annealing of solids or thermodynamic systems. In this method, the current state, energy equation, and ground state of a thermodynamic system are analogous to the current scheduling solution, objective function, and global optimum solution of the optimization problem. The SA algorithm uses the probability-based Metropolis acceptance rule to explore the search universe and leap away from the local optimum, which sets the probability of accepting weak solutions [56,57]. This rule is defined by

$$p^k = \exp\left[ -\frac{E^k - E_g}{K_{bo} T_k} \right] \tag{8}$$

where $p^k$ is the acceptance probability in the $k$th iteration; $E^k$ is the objective function value in the $k$th iteration; $E_g$ is the historical optimal objective function value; $K_{bo}$ is the Boltzmann coefficient; and $T_k$ is the annealing temperature in the $k$th iteration, which is initially set to a large value and then reduced to a small value via the following temperature-control function:

$$T_{k+1} = \alpha \times T_k \tag{9}$$

where $\alpha$ is the annealing coefficient, and its value interval is (0.8, 1.0). Thus with a gradual decrease in $T_k$, the acceptance probability of the inferior solution will approach 0.

### 2.2.3. SAPSO Algorithm

When the PSO algorithm is used to find the optimal solution for a model, the particles always chase the current optimal solution, which makes their speed close to zero and can cause the solution to fall into a local extreme point. To overcome this problem of precocious convergence, it is necessary to allow the algorithm to jump out of a local optimization and into other feasible regions when precocious convergence occurs. As the SA algorithm can accept a new state with a specified probability during the search process, even if there are multiple local optimal solutions to a problem, the algorithm can effectively prevent the final result from falling into a local extreme point. However, the SA algorithm has the disadvantages of a slow search speed in the later stages as well as low accuracy. Considering their advantages and disadvantages, the SAPSO algorithm was constructed in this study by combining the SA and PSO algorithms. Thus, the Boltzmann equation of the SA algorithm was incorporated into the iterative process of the PSO algorithm to effectively avoid the premature defects associated with the PSO algorithm while retaining its advantageously short local convergence time. The procedure of SAPSO algorithm is as follows:

Step 1: Let the iteration number $k = 1$, and set the initial population and parameters, including the initial population size *sizepop*, the spatial dimension of the population *dim*, initial position ${x_{jh}}^k$, initial speed ${v_{jh}}^k$, maximum number of iterations $N$, $w$, $c_1$, $c_2$, $T_k$, $\alpha$, and other parameters, in which $j$ = 1,2, ... , *sizepop*, $h$ = 1,2, ... , *dim*.

Step 2: Calculate the fitness value $fitness_j$ of each particle, and update the best historical position of the individual (${Pbest_j}^k$) and group (*Gbest*). Compare $fitness_j$ with ${Pbest_j}^k$; if the objective function is used to find the minimum, when $fitness_j < {Pbest_j}^k$, replace ${Pbest_j}^k$ with $fitness_j$, and when ${Pbest_j}^k < Gbest$, replace *Gbest* with ${Pbest_j}^k$; if the objective function is used to find the maximum, when $fitness_j > {Pbest_j}^k$, replace ${Pbest_j}^k$ with $fitness_j$, and when ${Pbest_j}^k > Gbest$, replace *Gbest* with ${Pbest_j}^k$.

Step 3: Use the Boltzmann equation, Equation (8), to calculate the acceptance probability of ${Pbest_j}^k$ at the current temperature $T_k$ as follows:

$$p\left(Pbest_j^k\right) = \exp\left(-\frac{fitness\left(Pbest_j^k\right) - fitness(Gbest)}{T_k}\right) \tag{10}$$

where $fitness({Pbest_j}^k)$ is the fitness value of ${Pbest_j}^k$, and $fitness(Gbest)$ is the fitness value of *Gbest*. Then, the fitness value *TF of* ${Pbest_j}^k$ is calculated as follows:

$$TF\left(Pbest_j^k\right) = \frac{p\left(Pbest_j^k\right)}{\sum_{j=1}^{sizepop} p\left(Pbest_j^k\right)} \tag{11}$$

Step 4: Update *Gbest* via the Metropolis method as follows:

$$Gbest = \begin{cases} Pbest_j^k & rand \le TF\left(Pbest_j^k\right) \\ Gbest & other \end{cases} \tag{12}$$

where *rand* is a random numbers taken in the range of (0, 1).

Step 5: Update the speeds and positions of the particles respectively using Equations (6) and (7).

Step 6: Apply the temperature control function given by Equation (9) to obtain a new temperature $T_{k+1}$.

Step 7: Let $k = k + 1$. If the iteration number $k \le N$, go to Step 2 to continue the iterative calculation; otherwise, end the iterative calculation.

#### 2.2.4. Procedure for Determining Optimal Operation Using the SAPSO Algorithm

When using the SAPSO algorithm to obtain the optimal operation model for a cascade reservoir system, the outflow of each reservoir is taken as the decision variable. A particle defines a specific outflow scheme. The procedure for solving the optimal cascade reservoir operation scheme using the SAPSO algorithm is as follows:

Step 1: Let the iteration number $k = 1$, and set the population parameters. The spatial dimension of the population *dim* is defined as the product of the number of reservoirs $M$ and the number of operation periods $T$; that is, $dim = m \times T$. The appropriate initial population size *sizepop* is then set along with the maximum number of iterations $N$, $w$, $c_1$, $c_2$, $T_k$, $\alpha$, and other parameters.

Step 2: Randomly generate the initial population, that is, the initial outflow hydrographs, as follows:

$$q_{jh}^{k} = q_{jh\min} + \left(q_{jh\max} - q_{jh\min}\right) \times rand \tag{13}$$

where $q_{jh}^{k}$, $q_{jh\max}$, and $q_{jh\min}$ are the outflow, upper limit of the outflow, and lower limit of the outflow, respectively, for the *h*th spatial dimension in the *j*th particle, where *j* = 1,2, ... , *sizepop,* and *h* = 1,2, ... , *dim*.

Step 3: Ascertain whether the population satisfies the constraint conditions by calculating the fitness value as follows:

$$fitness_j = fun\left(q_j^k\right) \tag{14}$$

where *fun* is the objective function of the optimal cascade reservoir flood-control operation model proposed in this study; $q_j^k$ is the outflow of the *j*th particle at iteration *k*.

Step 4: Update the best historical position of the individual ($Pbest_j{}^k$) and group (*Gbest*). Compare $fitness_j$ with $Pbest_j{}^k$; because the objective function employed in this study was used to find the minimum, when $fitness_j < Pbest_j{}^k$, replace $Pbest_j{}^k$ with $fitness_j$, and when $Pbest_j{}^k < Gbest$, replace *Gbest* with $Pbest_j{}^k$.

Step 5: Same as the Step 3 of the SAPSO algorithm, where *fitness* in Equation (10) is replaced by *fun*.

Step 6: Same as the Step 4 of the SAPSO algorithm.

Step 7: Update the speeds and positions of the particles respectively using Equations (6) and (7), where $x_{jh}^{k}$ and $x_{jh}^{k+1}$ in Equations (6) and (7) are replaced by $q_{jh}^{k}$ and $q_{jh}^{k+1}$, respectively.

Step 8: Same as the Step 6 of the SAPSO algorithm.

Step 9: Let $k = k + 1$. If the iteration number $k \leq N$, go to Step 3 to continue the iterative calculation; otherwise, output the optimal solution *Gbest*.

The procedure for determining optimal operation using the SAPSO algorithm is illustrated in Figure 1.

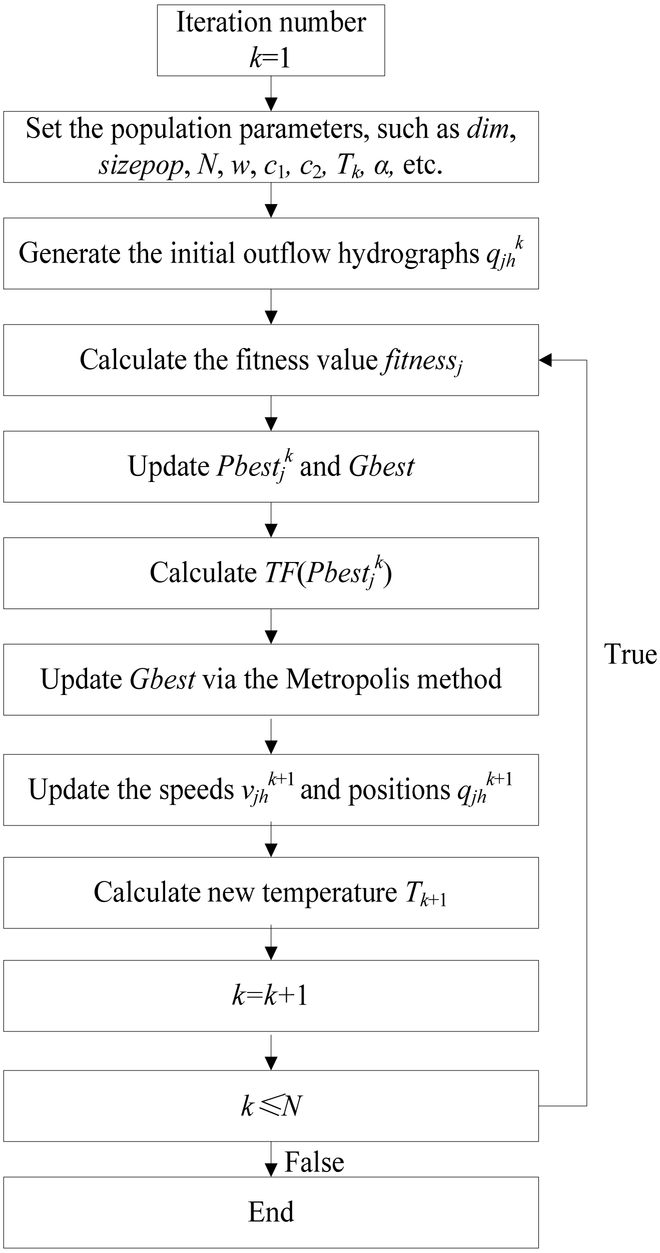


**Figure 1.** The flowchart of the procedure for determining optimal operation using the SAPSO algorithm.

## 3. Case Study

### *3.1. Study Area*

The Tianzhuang–Bashan cascade reservoir system was selected for the case study in this research. Bashan Reservoir is located in the middle to upper reaches of the main stream of the Yi River in the Huaihe River basin, China, and the Tianzhuang Reservoir is the only large reservoir in the upper reaches of the Yi River; these two reservoirs form the cascade reservoir system shown in Figure 2. They are both large, type II reservoirs with multi-year regulations used mainly to provide flood control and irrigation in combination with aquaculture, power generation, water supply, etc. The basic parameters of the reservoirs are listed in Table 2.

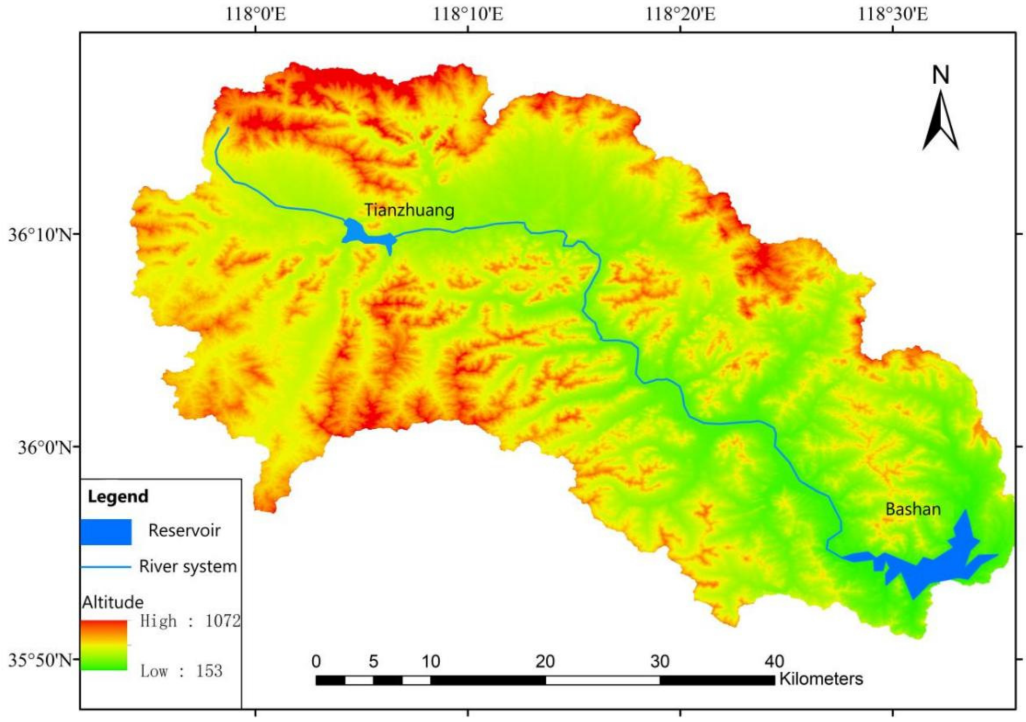


**Figure 2.** Watershed map of Tianzhuang–Bashan cascade reservoir system.

**Table 2.** Basic parameters of the two reservoirs.

| Items | Unit | Bashan Reservoir | Tianzhuang Reservoir |
|---|---|---|---|
| Catchment area | km$^2$ | 1782 | 424 |
| Design standard | % | 1 | 1 |
| Check standard | % | 0.01 | 0.01 |
| Checked flood level | m | 182.61 | 315.07 |
| Designed flood level | m | 178.22 | 312.38 |
| Normal water level | m | 176.27 | 310.64 |
| Dead water level | m | 161.07 | 293.64 |
| Total storage | $10^8$ m$^3$ | 5.28 | 1.3057 |
| Active storage | $10^8$ m$^3$ | 2.67 | 0.6840 |
| Dead storage | $10^8$ m$^3$ | 0.14 | 0.0173 |

Two control discharges and a high-volume discharge state were established for each reservoir to ensure safety downstream. For the Bashan Reservoir, when the water level $Z \leq 179.02$ m, the control discharge is 2000 m$^3$/s; when 179.02 m $< Z \leq$ 179.90 m, the control discharge is 3120 m$^3$/s; and when $Z > 179.90$ m, the spillway sluices are completely opened. For the Tianzhuang Reservoir, when the water level $Z \leq 311.78$ m, the control discharge is 600 m$^3$/s; when 311.78 m $< Z \leq$ 312.33 m, the control discharge is 1000 m$^3$/s; and when $Z > 312.33$ m, the spillway sluices are completely opened.

### *3.2. Data Processing and Parameter Setting*

Data were collected describing two floods of the Tianzhuang–Bashan cascade reservoir system on 31 July 1964 and 13 August 1974, including the water level, storage capacity, and outflow data for both reservoirs. Based on these data, the inflow for each reservoir was calculated using the water balance equation given by Equation (2). According to the observations, the duration of the outflow from Tianzhuang Reservoir to Bashan Reservoir through river routing is 6 h, so $t'$ in Equation (3) was set to 6 h. At the same time, the relationships between the water level and storage capacity and between the water level and outflow of the each reservoir were also obtained. In summary, the collected data met the modeling requirements for the optimal cascade reservoir operation model.

According to [58] and based on the results many tests of the PSO and SAPSO algorithms, the parameters of the two algorithms were determined and applied in this study as shown in Table 3 to demonstrate the abilities of the proposed SAPSO algorithm.

**Table 3.** Algorithm parameters.

| Parameters | PSO Algorithm | SAPSO Algorithm |
|---|---|---|
| *sizepop* | 100 | 100 |
| $N$ | 6000 | 6000 |
| $w$ | 0.8 | 0.8 |
| $c_1$ | 0.5 | 0.5 |
| $c_2$ | 0.5 | 0.5 |
| $T_a$ | | $10^6$ |
| $\alpha$ | | 0.9 |

## 4. Results and Discussion

### 4.1. Results

First, the optimal operation model of the Tianzhuang–Bashan cascade reservoir system was established according to the procedure in Section 2.1. In Equation (1); $M$ equals 2, $q_1(t)$ and $q_2(t)$ are the inflows of Tianzhuang and Bashan Reservoir, respectively; and $R_2(t)$ is the inflow from Tianzhuang Reservoir to Bashan Reservoir, obtained by subtracting the outflow of Tianzhuang Reservoir at $t-6$ h from the inflow of Bashan Reservoir. Then, the PSO and SAPSO (https://github.com/regicsf2010/SAPSO, accessed on 10 September 2021) algorithms were compiled using the MATLAB software to solve the optimal operation schemes for the 31 July 1964 and 13 August 1974 floods. The results were compared with the measured values as shown in Figures 3–6. The maximum outflows and water levels are listed in Tables 4 and 5, respectively.

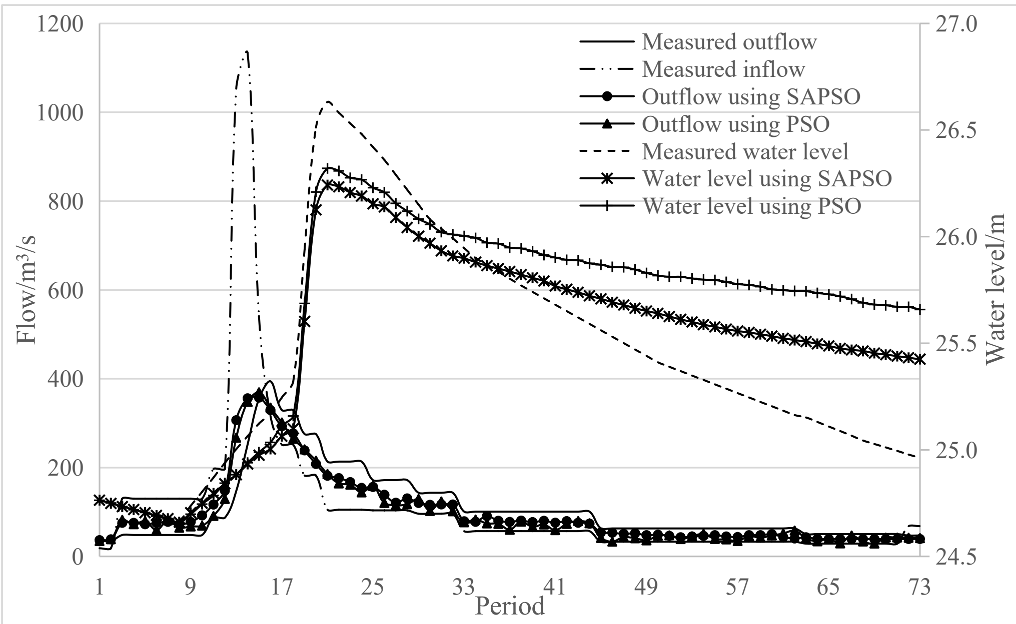


**Figure 3.** Operation hydrographs of Tianzhuang Reservoir for the 31 July 1964 flood.

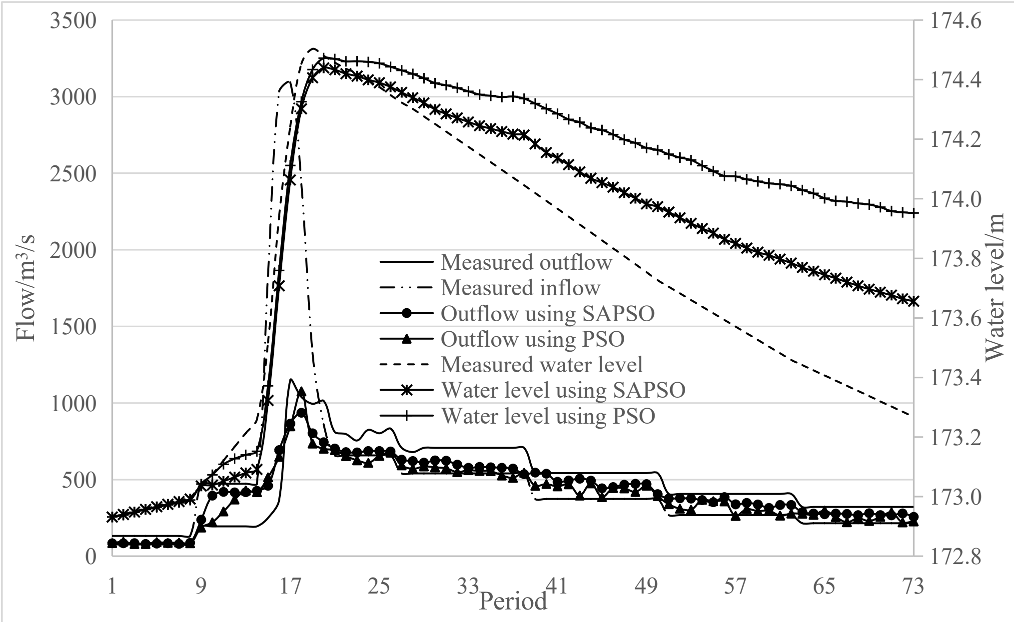


**Figure 4.** Operation hydrographs of Bashan Reservoir for the 31 July 1964 flood.

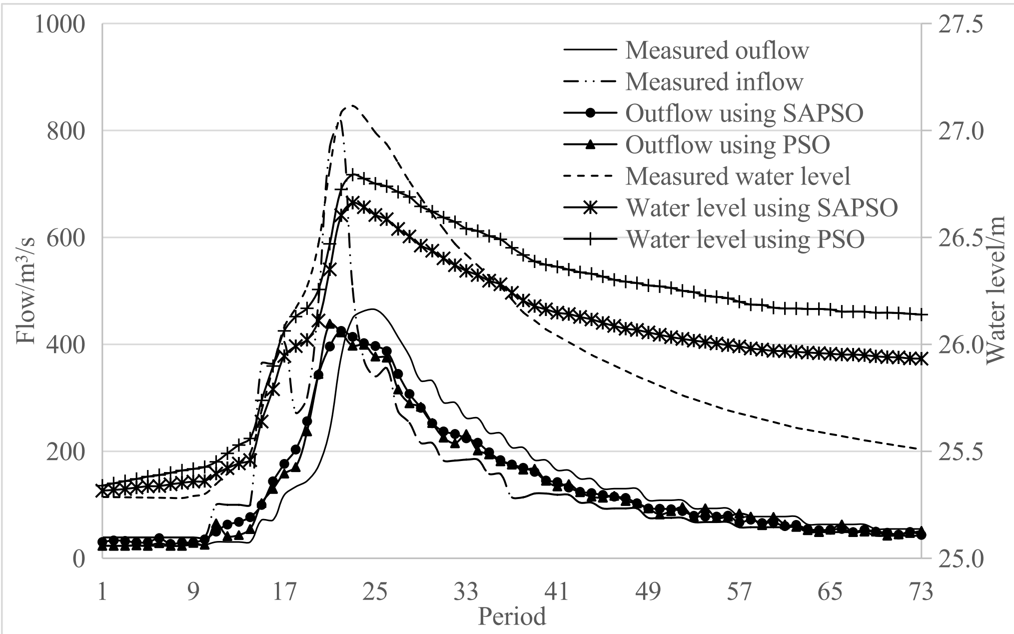


**Figure 5.** Operation hydrographs of Tianzhuang Reservoir for the 13 August 1974 flood.

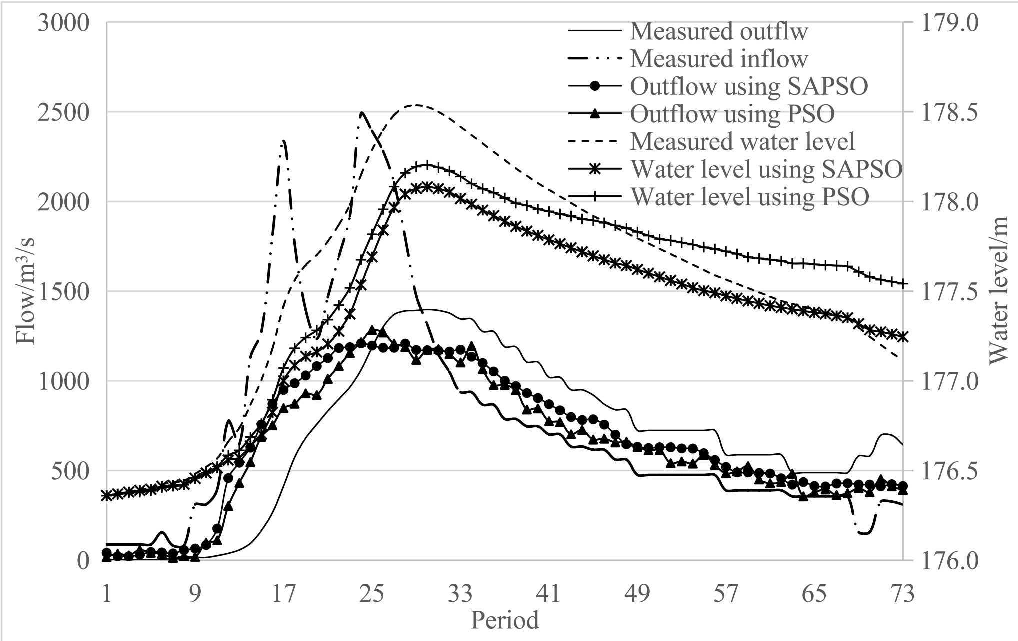


**Figure 6.** Operation hydrographs of Bashan Reservoir for the 13 August 1974 flood.

**Table 4.** Comparison of operating results for the 31 July 1964 flood.

| Item | | Measured Data | Operation Results Using PSO Algorithm | Operation Results Using SAPSO Algorithm |
|---|---|---|---|---|
| Tianzhuang Reservoir | Maximum outflow ($m^3$/s) | 394.36 | 369.87 | 357.61 |
| | Maximum water level (m) | 26.63 | 26.32 | 26.24 |
| Bashan Reservoir | Maximum outflow ($m^3$/s) | 1149.34 | 1056.01 | 936.53 |
| | Maximum water level (m) | 174.50 | 174.47 | 174.44 |

**Table 5.** Comparison of operating results for the 13 August 1974 flood.

| Item | | Measured Data | Operation Results Using PSO Algorithm | Operation Results Using SAPSO Algorithm |
|---|---|---|---|---|
| Tianzhuang Reservoir | Maximum outflow ($m^3$/s) | 465.00 | 438.48 | 425.03 |
| | Maximum water level (m) | 27.11 | 26.79 | 26.66 |
| Bashan Reservoir | Maximum outflow ($m^3$/s) | 1397.50 | 1269.07 | 1209.00 |
| | Maximum water level (m) | 178.54 | 178.20 | 178.08 |

(1) Comparing the maximum outflows shown for the two floods in Tables 3 and 4, the measured maximum outflows of the two reservoirs were the largest, followed by those under the operation scheme obtained using the PSO algorithm, followed by those under the operation scheme obtained using the proposed SAPSO algorithm. The maximum outflow of Tianzhuang Reservoir when operated according to the PSO-obtained solution decreased by 6.2% and 5.7% compared with the measured values in the 31 July 1964 and the 13 August 1974 floods, respectively; the maximum outflow of Bashan Reservoir when operated according to the PSO-obtained solution decreased by 8.1% and 9.2% compared with the measured values in the 31 July 1964 and 13 August 1974 floods, respectively. Notably, the maximum outflow of Tianzhuang Reservoir when operated according to the SAPSO-obtained solution decreased by 9.3% and 8.6% compared with the measured values in the 31 July 1964 and 13 August 1974 floods, respectively; the maximum outflow of Bashan Reservoir when operated according to the SAPSO-obtained solution decreased by 18.5% and 13.5% compared with the measured value in the 31 July 1964 and 13 August 1974 floods,

respectively. Thus, both the PSO and SAPSO algorithms reduced the maximum outflow of the two reservoirs, with the proposed SAPSO algorithm providing superior performance.

(2) For both floods, the measured maximum water levels of the two reservoirs were the largest, followed by those of the PSO-obtained operation scheme, then by those of the SAPSO-obtained operation scheme. The maximum water levels of Tianzhuang Reservoir when using the PSO-based strategy were 0.31 m and 0.32 m lower than the measured values during the 31 July 1964 and 13 August 1974 floods, respectively, and those of Bashan Reservoir were 0.03 m and 0.34 m lower than the measured values, respectively. The maximum water levels of Tianzhuang Reservoir when using the SAPSO-based strategy were 0.39 m and 0.45 m lower than the measured values during the 31 July 1964 and 13 August 1974 floods, respectively, and those of Bashan Reservoir were 0.06 m and 0.46 m lower than the measured values, respectively. Thus, it can be observed that the maximum water levels obtained when using the optimal operation schemes based on the PSO and SAPSO algorithms were smaller than the measured values, with the maximum water level of the latter being the smallest.

(3) The convergence processes for the SAPSO and PSO algorithms are shown in Figures 7 and 8, respectively. It can be seen that in the process of obtaining the optimal operation schemes for the 31 July 1964 and 13 August 1974 floods, the PSO algorithm fell into a local optimal solution at 1676 and 1338 iterations, respectively. However, the SAPSO algorithm tended to be stable and reached a minimum at 5690 and 5993 iterations, respectively. The minimum values of the PSO and SAPSO algorithms objective functions for the 31 July 1964 flood were $4.77 \times 10^9$ and $4.65 \times 10^9$, respectively, while those for the 13 August 1974 flood were $1.36 \times 10^{10}$ and $1.34 \times 10^{10}$, respectively. Thus, the minimum values of the objective function obtained using the proposed SAPSO algorithm were less than those obtained using the PSO algorithm. In summary, SAPSO algorithm can not only effectively avoid the problem of falling into a local optimal solution in the later stage of the optimization process when using the PSO algorithm but also provide superior objective function values.

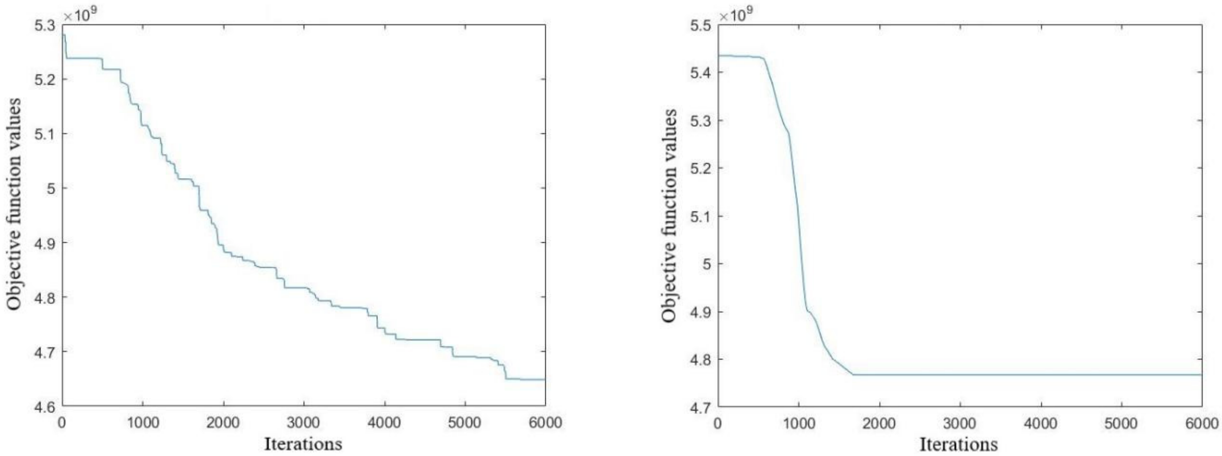


(**a**) (**b**)

**Figure 7.** Convergence processes for the 31 July 1964 flood using the (**a**) SAPSO and (**b**) PSO algorithms.

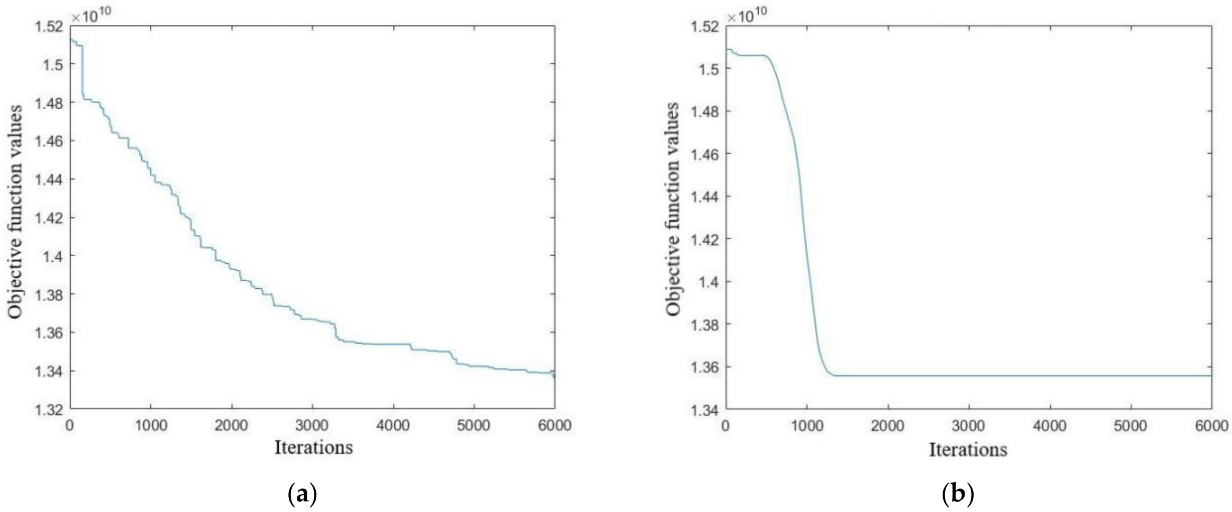


**Figure 8.** Convergence processes for the 13 August 1974 flood using the (**a**) SAPSO and (**b**) PSO algorithms.

### *4.2. Discussion*

#### 4.2.1. The Comparison of Outflows

From the three outflow hydrographs shown in Figures 3–6, it can be observed that when the flood waters were rising, the optimal operation schemes obtained using PSO and SAPSO algorithms increased the outflow ahead of time compared to the measured operation scheme; this is quite obvious for the Bashan Reservoir in particular. For example, during the 31 July 1964 and 13 August 1974 floods, the operation schemes using either algorithm increased the outflow 4 h and 7 h earlier, respectively. Increasing the outflow in advance can ensure the maximum available reservoir storage capacity and reduce the maximum outflow under the same flood conditions; this is also the main reason why the maximum outflows under the two optimal operation schemes were smaller than the measured values. Comparing the three outflow hydrographs, those corresponding to the two optimization schemes show that the outflows as the floods rose were larger than the measured values, the peak outflow times appeared earlier than for the measured outflows, and the outflows as the floods receded were smaller than the measured values. Comparing the outflow hydrographs obtained using the two optimization algorithms, the SAPSO-based outflow hydrographs were smoother than the PSO-based outflow hydrographs whether the floods were rising or receding, and except for the maximum outflow, the PSO-obtained outflows were smaller than the SAPSO-obtained outflows. In addition, the fluctuations of the PSO-obtained outflow hydrographs were quite serious, indicating that they fell into local optimal solutions during optimization.

Comparing the water-level hydrographs shown in Figures 3–6, the water levels obtained using the operating strategies based on the two optimization algorithms were consistently lower than the measured values until reaching the maximum water level; this is particularly obvious for the 13 August 1974 flood at Bashan Reservoir. After achieving the maximum water level, the water levels of the two algorithms intersected with the measured values at a later time for the 13 August 1974 flood than for the 31 July 1964 flood; this was caused by the combined influence of the maximum inflow and the algorithm-derived operating strategy. The appearance times of the highest water levels obtained using the operating strategies derived using the two optimization algorithms were mostly consistent with the measured value. However, the measured water levels at the ends of the two floods were lower than those obtained when using the evaluated optimal operation methods; this indicates that the two optimization algorithms more effectively utilized flood resources.

Based on the study by Farzin et al. [59], the GA was used in the flow analysis. Comparison of routings with three outflow hydrographs for each flood and each reservoir indicated that the SAPSO algorithm reaches an improved routing. The results were so similar because of the accurate sensitivity analysis considered in various algorithms for the objective function and different parameters. Although the changes of outflows can be seen clearly in Figures 9 and 10, the appearance times of maximum outflow using the three algorithms were mostly consistent. An interesting fact is that the GA's outflow hydrographs of Bashan reservoir show a highly variable outflow peak compared with the performance of PSO and SAPSO algorithms. The reason of this fact is that the GA uses probabilistic transition rules to guide the search direction but does not use deterministic search rules, and the search process does not directly act on variables. Derrac et al. [60] suggested that multiple comparisons tests must be used when a statistical comparison of the results is reported among various algorithms. However, this study prefers to compare the performance of SAPSO and PSO algorithms, while the GA was only chosen as another algorithm for simple comparison.

#### 4.2.2. The Computational Performance

From the optimization results, SAPSO generally improves the operation policy. From the convergence processes, the dynamic probability optimization of the SA algorithm reduces the convergence speed in the early stage of convergence, which may be related to the fact that the dynamic discovery probability changes the balance between global and local search in the evolution process of the algorithm. In terms of algorithm complexity, the dynamic probability optimization does not change the complexity of the proposed algorithm, so the optimization time is basically not affected. In intelligent algorithms, the optimization results can be further improved by increasing the population size or the number of iterations, but it also occupies more computer memory and prolongs the optimization time.

It can be seen that in the process of obtaining the optimal operation schemes for the 31 July 1964 and 13 August 1974 floods, the PSO algorithm fell into a local optimal solution at 1676 and 1338 iterations, respectively. However, the SAPSO algorithm tended to be stable and reached a minimum at 5690 and 5993 iterations, respectively. The probabilistic optimization mechanism of the SA algorithm determines that it has a significant performance in overcoming the "prematurity" of PSO. At the same time, it ensures that the PSO algorithm can still maintain good population diversity in the later stage of evolution, so the SAPSO algorithm does not easily fall into local optimal solution. After a certain number of iterations, the SAPSO algorithm can converge to the global optimal solution.

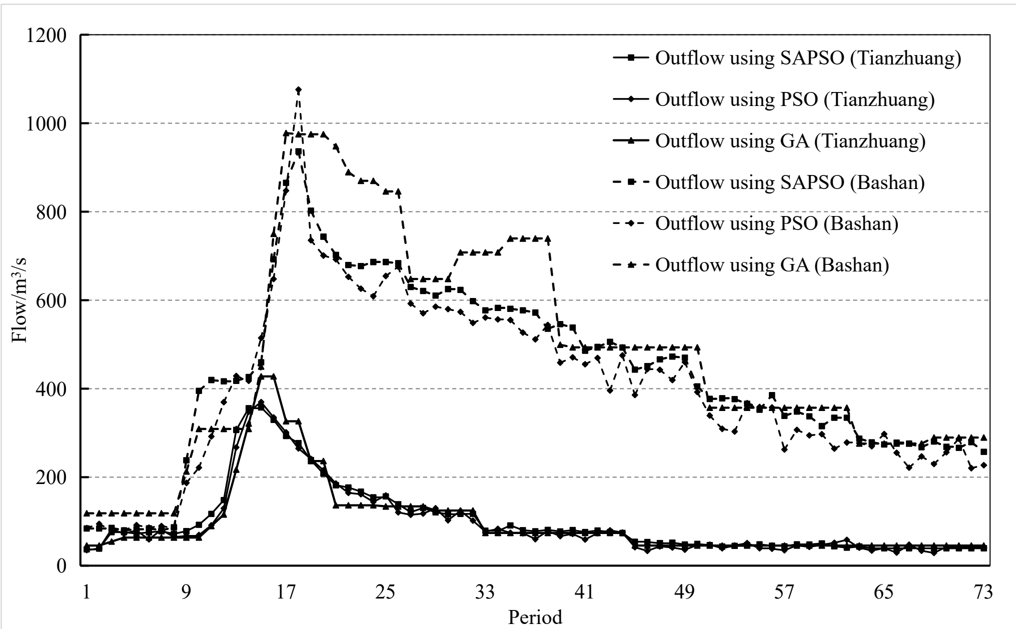


**Figure 9.** Outflow hydrographs for the 31 July 1964 flood using the SAPSO, PSO, and GA algorithms.

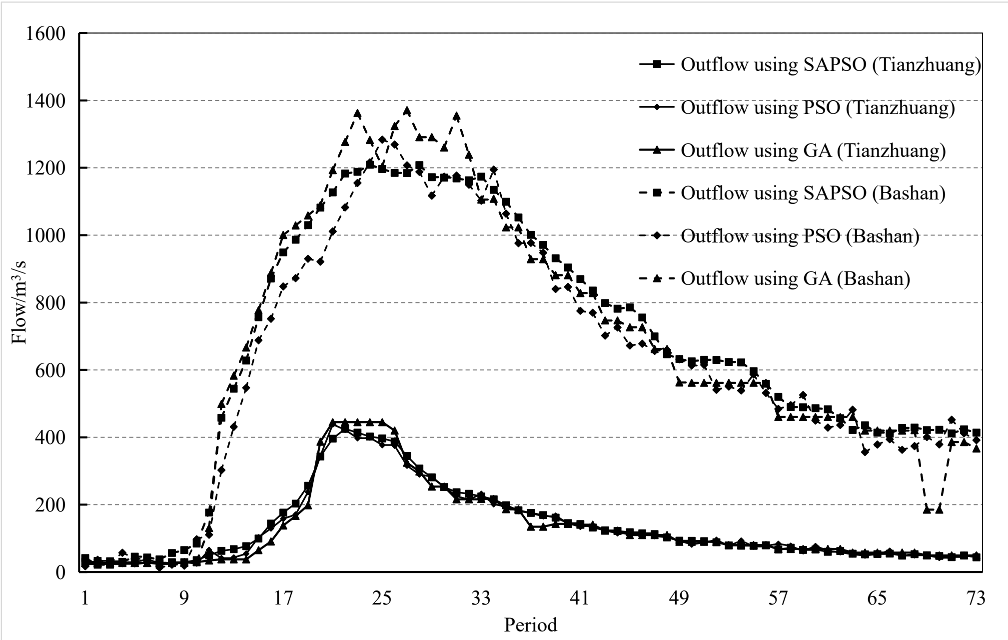


**Figure 10.** Outflow hydrographs for the 13 August 1974 flood using the SAPSO, PSO, and GA algorithms.

## 5. Conclusions

Taking the maximum reduction of the flood peak as the objective function, a cascade reservoir system flood-control operation optimization model was constructed and solved using the SAPSO algorithm proposed in this study. The proposed approach was then applied to formulate an optimal operation scheme for the Tianzhuang–Bashan cascade reservoir system. The following conclusions were drawn from this study:

(1) The maximum outflows and water levels of the optimal operation schemes obtained using the SAPSO algorithm were smaller than the measured values and those of the optimal operation scheme obtained using the PSO algorithm. Therefore, the SAPSO algorithm was not only able to provide an operation scheme that maximized safety in the downstream flood control areas, but it also took into account the flood-control safety of the reservoirs themselves as well as their upstream areas.

(2) The optimal operation schemes obtained using the PSO and SAPSO algorithms both increased the outflow in advance of the flood. Indeed, the outflow hydrographs for the two optimization schemes indicated that the outflows as the floods rose were larger, the peak outflows appeared earlier, and the outflows as the floods receded were smaller compared to the measured values. Except for the maximum outflow, the outflows provided by the PSO-based scheme were generally smaller than those provided by the SAPSO-based scheme. Furthermore, the water levels obtained using the PSO- and SAPSO-based schemes were lower than the measured values when the floods rose, whereas those at the end of flood regulation were higher than the measured values. In summary, the two optimization algorithms were not only able to ensure the safety of the reservoirs and downstream flood control areas but also realized the effective utilization of flood-water resources.

(3) Comparing the convergence processes of the SAPSO and PSO algorithms, it was determined that the SAPSO algorithm effectively avoided the problem of falling into a local optimal solution during the later stages of the optimization process, as occurred when using the PSO algorithm, and provided a superior objective function value.

Therefore, the cascade reservoir flood-control optimal operation model and SAPSO algorithm proposed in this study provide a new approach that can be confidently applied to the flood-control optimization of cascade reservoir systems. It is well known that the availability of the new proposed algorithm depends on the applicability and performance in the actual events. However, only two floods of one cascade reservoir system were optimized using SAPSO algorithm in this study, and it should be applied to more reservoir systems and more floods in the future to prove the applicability of this algorithm. Considering the fact that the initial conditions that guarantee the reliability of the parametric tests are not satisfied, a nonparametric test is encouraged due to the necessity of analyzing results obtained by evolutionary or swarm intelligence algorithms for continuous optimization problems in multi-problem analysis in the future [60].

**Author Contributions:** Conceptualization, Y.D. and Q.Q.; methodology, Y.D. and H.M.; investigation, Y.D. and H.W.; data curation, J.W., H.M., S.L. and X.L.; writing—original draft preparation, H.M., H.W., Y.D. and J.P.; writing—review and editing, Q.Q.; funding acquisition, Y.D. and Q.Q. All authors have read and agreed to the published version of the manuscript.

**Funding:** This research was funded by the Key Technology Research and Development Program of Shandong Province, grant numbers 2019GSF111043; the Natural Science Foundation of Shandong Province, grant numbers ZR2021ME058; the Open Research Fund of State Key Laboratory of Simulation and Regulation of Water Cycle in River Basin (China Institute of Water Resources and Hydropower Research), grant numbers IWHR-SKL-KF202118; Shandong science and technology small and medium-sized enterprise innovation ability improvement project, grant numbers 2021TSGC1082.

**Institutional Review Board Statement:** Not applicable.

**Informed Consent Statement:** Not applicable.

**Data Availability Statement:** The datasets used and/or analyzed during the current study are available from the corresponding author upon reasonable request.

**Acknowledgments:** We express our deepest gratitude to Xin Chen for his help in drawing the watershed map and to the reservoir management and operation centers for their help in data support.

**Conflicts of Interest:** The authors declare no conflict of interest.

## References

1. Academy of Disaster Reduction and Emergency Management, Ministry of Emergency Management-Ministry of Education, National Disaster Reduction Center of China. *2020 Global Natural Disaster Assessment Report*; National Disaster Reduction Center of China: Beijing, China, 2021.
2. Bellman, R. *Dynamic Programming*; Princeton University Press: Princeton, NJ, USA, 1957.
3. Howson, H.R.; Sancho, N.G.F. A new algorithm for the solution of multi-state dynamic programming problems. *Math. Program.* **1975**, *8*, 114–116. [CrossRef]
4. Manne, A.S. Product mix alternatives: Flood control, electric power and irrigation. *Int. Econ. Rev.* **1962**, *8*, 30–54. [CrossRef]
5. Niu, W.J.; Feng, Z.K.; Cheng, C.T. Min-Max linear programming model for multireservoir system operation with power deficit aspect. *J. Water Resour. Plan. Manag.* **2018**, *144*, 06018006.1–06018006.5. [CrossRef]
6. Su, C.; Yuan, W.; Cheng, C.; Wang, P.; Sun, L.; Zhang, T. Short-term generation scheduling of cascade hydropower plants with strong hydraulic coupling and head-dependent prohibited operating zones. *J. Hydrol.* **2020**, *591*, 125556. [CrossRef]
7. Dogan, M.S.; Lund, J.; Azuara, J.M. Hybrid linear and nonlinear programming model for hydropower reservoir optimization. *J. Water Resour. Plan. Manag.* **2021**, *147*, 06021001. [CrossRef]
8. Ji, C.; Li, C.; Wang, B.; Liu, M.; Wang, L. Multi-stage dynamic programming method for short-term cascade reservoirs optimal operation with flow attenuation. *Water Resour. Manag.* **2017**, *31*, 4571–4586. [CrossRef]
9. Wu, X.; Cheng, C.; Lund, J.R.; Niu, W.; Miao, S. Stochastic dynamic programming for hydropower reservoir operations with multiple local optima. *J. Hydrol.* **2018**, *564*, 712–722. [CrossRef]
10. He, S.; Guo, S.; Chen, K.; Deng, L.; Liao, Z.; Xiong, F.; Yin, J. Dataset for reservoir impoundment operation coupling parallel dynamic programming with importance sampling and successive approximation. *Data Brief* **2019**, *26*, 104440. [CrossRef]
11. Feng, Z.; Wen, J.; Xiong, C.; Wang, J.; Wang, S.; Song, Z. An effective three-stage hybrid optimization method for source-network-load power generation of cascade hydropower reservoirs serving multiple interconnected power grids. *J. Clean. Prod.* **2018**, *246*, 119035. [CrossRef]
12. Ma, Y.; Zhong, P.; Xu, B.; Zhu, F.; Lu, Q.; Han, W. Spark-based parallel dynamic programming and particle swarm optimization via cloud computing for a large-scale reservoir system. *J. Hydrol.* **2021**, *598*, 126444. [CrossRef]
13. Feng, Z.; Niu, W.; Cheng, C.; Lund, J.R. Optimizing hydropower reservoirs operation via an orthogonal progressive optimality algorithm. *J. Water Resour. Plan. Manag.* **2018**, *144*, 4018001.1. [CrossRef]
14. Jiang, Z.; Ji, C.; Qin, H.; Feng, Z. Multi-stage progressive optimality algorithm and its application in energy storage operation chart optimization of cascade reservoirs. *Energy* **2018**, *148*, 309–323. [CrossRef]

15. Zhou, C.; Sun, N.; Chen, L.; Ding, Y.; Zhou, J.; Zha, G.; Luo, G.; Dai, L.; Yang, X. Optimal Operation of Cascade Reservoirs for Flood Control of Multiple Areas Downstream: A Case Study in the Upper Yangtze River Basin. *Water* **2018**, *10*, 1250. [CrossRef]
16. Chen, J. Long-term joint operation of cascade reservoirs using enhanced progressive optimality algorithm and dynamic programming hybrid approach. *Water Resour. Manag.* **2021**, *35*, 2265–2279. [CrossRef]
17. Ji, C.; Liu, Y.; Wang, Y.; Zhang, Y.; Xie, Y. Considering water propagation impact in short-term optimal operation of cascade reservoirs using nested progressive optimality algorithm. *J. Hydrol.* **2021**, *602*, 126764. [CrossRef]
18. Albo-Salih, H.; Mays, L. Testing of an optimization-simulation model for real-time flood operation of river-reservoir systems. *Water* **2021**, *13*, 1207. [CrossRef]
19. Jhong, B.C.; Fang, H.T.; Huang, C.C. Assessment of Effective Monitoring Sites in a Reservoir Watershed by Support Vector Machine Coupled with Multi-Objective Genetic Algorithm for Sediment Flux Prediction during Typhoons. *Water Resour. Manag.* **2021**, *35*, 2387–2408. [CrossRef]
20. Lin, N.M.; Tian, X.; Rutten, M.; Abraham, E. Multi-objective model predictive control for real-time operation of a multi-reservoir system. *Water* **2020**, *12*, 1898. [CrossRef]
21. Liu, D.; Huang, Q.; Yang, Y.; Liu, D.; Wei, X. Bi-objective algorithm based on NSGA-II framework to optimize reservoirs operation. *J. Hydrol.* **2020**, *585*, 124830. [CrossRef]
22. Shaikh, S.A. Application of artificial neural network for optimal operation of a multi-purpose multi-reservoir system, II: Optimal solution and performance evaluatio. *Sustain. Water Resour. Manag.* **2020**, *6*, 115–123. [CrossRef]
23. Zhang, D.; Lin, J.; Peng, Q.; Wang, D.; Yang, T.; Sorooshian, S.; Liu, X.; Zhuang, J. Modeling and simulating of reservoir operation using the artificial neural network, support vector regression, deep learning algorithm. *J. Hydrol.* **2018**, *565*, 720–736. [CrossRef]
24. Dahmani, S.; Yebdri, D. Hybrid algorithm of particle swarm optimization and grey wolf optimizer for reservoir operation management. *Water Resour. Manag.* **2020**, *34*, 4545–4560. [CrossRef]
25. Kumar, D.N.; Reddy, M.J. Ant colony optimization for multi-purpose reservoir operation. *Water Resour. Manag.* **2020**, *6*, 879–898. [CrossRef]
26. Afshar, A.; Sharifi, F.; Jalali, M.R. Applying the non-dominated archiving multi-colony ant algorithm for multi-objective optimization: Application to multi-purpose reservoir operation. *Eng. Optim.* **2009**, *41*, 313–325. [CrossRef]
27. Teegavarapu, R.S.V.; Simonovic, S.P. Optimal operation of reservoir systems using simulated annealing. *Water Resour. Manag.* **2002**, *16*, 401–428. [CrossRef]
28. Azizipour, M.; Sattari, A.; Afshar, M.H.; Goharian, E. Optimal hydropower operation of multi-reservoir systems: Hybrid cellular automata-simulated annealing approach. *J. Hydroinform.* **2020**, *22*, 168. [CrossRef]
29. Qi, Y.; Liang, B.; Sun, Y.; Luo, J.; Miao, Q. A Memetic Multi-objective Immune Algorithm for Reservoir Flood Control Operation. *Water Resour. Manag.* **2016**, *30*, 2957–2977. [CrossRef]
30. Qi, Y.; Bao, L.; Ma, X.; Miao, Q.; Li, X. Self-adaptive multi-objective evolutionary algorithm based on decomposition for large-scale problems: A case study on reservoir flood control operation. *Inf. Sci.* **2016**, *367–368*, 529–549. [CrossRef]
31. Zhang, X.; Luo, J.; Sun, X.; Xie, J. Optimal reservoir flood operation using a decomposition-based multi-objective evolutionary algorithm. *Eng. Optim.* **2019**, *51*, 42–62. [CrossRef]
32. Liu, Y.; Qin, H.; Mo, L.; Wang, Y.; Chen, D.; Pang, S.; Yin, X. Hierarchical flood operation rules optimization using multi-objective cultured evolutionary algorithm based on decomposition. *Water Resour. Manag.* **2019**, *33*, 337–354. [CrossRef]
33. Lai, H.J.; Li, X.Y.; Zhang, L.; Zhou, Z.J.; Jing, Y.W. Improved FOA for optimal dispatch of cascade reservoirs. *Water Resour. Power* **2013**, *31*, 74–76.
34. Salman, A.; Engelbrecht, A.P.; Omran, M.G.H. Empirical analysis of self-adaptive differential evolution. *Eur. J. Operat. Res.* **2007**, *183*, 785–804. [CrossRef]
35. Jahandideh-Tehrani, M.; Bozorg-Haddad, O.; Loáiciga, H.A. Application of particle swarm optimization to water management: An introduction and overview. *Environ. Monit. Assess.* **2020**, *192*, 281. [CrossRef]
36. Chau, K.W. A split-step particle swarm optimization algorithm in river stage forecasting. *J. Hydrol.* **2007**, *346*, 131–135. [CrossRef]
37. Ghorbani, M.A.; Kazempour, R.; Chau, K.W.; Shamshirband, S.; Ghazvinei, P.T. Forecasting pan evaporation with an integrated artificial neural network quantum-behaved particle swarm optimization model: A case study in Talesh, northern Iran. *Eng. Appl. Comput. Fluid Mech.* **2018**, *12*, 724–737. [CrossRef]
38. Niu, W.J.; Feng, Z.K.; Cheng, C.T.; Zhou, J.Z. Forecasting daily runoff by extreme learning machine based on quantum-behaved particle swarm optimization. *J. Hydrol. Eng.* **2018**, *23*, 04018002. [CrossRef]
39. Afshar, A.; Shojaei, N.; Sagharjooghifarahani, M. Multiobjective calibration of reservoir water quality modeling using multiobjective particle swarm optimization(MOPSO). *Water Resour. Manag.* **2013**, *27*, 1931–1947. [CrossRef]
40. Kisi, O.; Keshavarzi, A.; Shiri, J.; Zounemat-Kermani, M.; Omran, E.E. Groundwater quality modeling using neuro-particle swarm optimization and neuro-differential evolution techniques. *Hydrol. Res.* **2017**, *48*, 1508–1519. [CrossRef]
41. Ehteram, M.; Othman, F.B.; Yaseen, Z.M.; Afan, H.A.; Allawi, M.F.; Malek, M.B.A.; Ahmed, A.N.; Shahid, S.; Singh, V.P.; El-Shafie, A. Improving the Muskingum flood routing method using a hybrid of particle swarm optimization and bat algorithm. *Water* **2018**, *10*, 807. [CrossRef]
42. Ezzeldin, R.; Djebedjian, B.; Saafan, T. Integer discrete particle swarm optimization of water distribution networks. *J. Pipeline Syst. Eng. Pract.* **2013**, *5*, 04013013. [CrossRef]

43. Sedki, A.; Ouazar, D. Hybrid particle swarm optimization and differential evolution for optimal design of water distribution systems. *Adv. Eng. Inform.* **2012**, *26*, 582–591. [CrossRef]
44. Kumar, D.N.; Reddy, M.J. Multipurpose reservoir operation using particle swarm optimization. *J. Water Resour. Plan. Manag.* **2007**, *133*, 192–201. [CrossRef]
45. Hojati, A.; Monadi, M.; Faridhosseini, A.; Mohammadi, M. Application and comparison of NSGA-II and MOPSO in multi-objective optimization of water resources systems. *J. Hydrol. Hydromech.* **2018**, *66*, 323–329. [CrossRef]
46. Guo, X.; Hu, T.; Wu, C.; Zhang, T.; Lv, Y. Multiobjective optimization of the proposed multi-reservoir operating policy using improved NSPSO. *Water Resour. Manag.* **2013**, *27*, 2137–2153. [CrossRef]
47. Zhong, D.; Dong, Z.; Zhao, Y.; Xu, W.; Guan, X. Cascade reservoir optimal operation based on chaotic particle swarm optimization. In *Advances in Computer Science Research, Proceedings of the 2017 2nd Joint International Information Technology, Mechanical and Electronic Engineering Conference, Chongqing, China, 4 October–5 October 2017*; Atlantis Press: Paris, France, 2017.
48. Yaseen, Z.M.; Ehteram, M.; Hossain, S.; Fai, C.M.; Koting, S.B.; Mohd, N.S.; Jaafar, W.Z.B.; Afan, H.A.; Hin, L.S.; Zaini, N.; et al. A novel hybrid evolutionary data-intelligence algorithm for irrigation and power production management: Application to multipurpose reservoir systems. *Water* **2019**, *11*, 1953. [CrossRef]
49. Trivedi, M.; Shrivastava, R. Derivation and performance evaluation of optimal operating policies for a reservoir using a novel PSO with elitism and variational parameters. *Urban Water J.* **2020**, *17*, 774–784. [CrossRef]
50. Mahdi, S.; Bithin, D.; Zeynab, F. Linking ecohydraulic simulation and optimization system for mitigating economic and environmental losses of reservoirs. *AQUA-Water Infrastruct. Ecosyst. Soc.* **2022**, *71*, 229–247.
51. Xu, B.; Zhong, P.; Stanko, Z.; Zhao, Y.; Yeh, W.W.G. A multiobjective short-term optimal operation model fora cascade system of reservoirs considering the impact on long-term energy production. *Water Resour. Res.* **2015**, *51*, 3353–3369. [CrossRef]
52. Ge, X.; Zhang, L.; Shu, J.; Xu, N. Short-term hydropower optimal scheduling considering the optimization of water time delay. *Electr. Power Syst. Res.* **2014**, *110*, 188–197. [CrossRef]
53. Wang, W.C.; Lei, G.J.; Yin, H.; Liu, H.M. Optimal dispatch model of reservoir flood control based on SSO algorithm. *Water Resour. Power* **2015**, *33*, 48–51.
54. Zou, Q.; Wang, X.M.; Li, A.Q.; He, X.C.; Lou, B. Optimal operation of flood control for cascade reservoirs based on parallel chaotic quantum particle swarm optimization. *J. Hydraul. Eng.* **2016**, *47*, 967–976.
55. Kennedy, J.; Eberhart, R. Particle swarm optimization. In Proceedings of the IEEE International Conference on Neural Networks, Perth, WA, Australia, 27 November–1 December 1995; IEEE: New York, NY, USA, 1995; pp. 1942–1948.
56. Kirkpatrick, S.; Gelatt, C.D.; Vecchi, M.P. Optimization by simulated annealing. *Science* **1983**, *220*, 671–680. [CrossRef] [PubMed]
57. Haznedar, B.; Kalinli, A. Training ANFIS structure using simulated annealing algorithm for dynamic systems identification. *Neurocomputing* **2018**, *302*, 66–74. [CrossRef]
58. Behnamian, J.; Ghomi, S.F. Development of a PSO-SA hybrid metaheuristic for a new comprehensive regression model to time-series forecasting. *Expert Syst. Appl.* **2009**, *37*, 974–984. [CrossRef]
59. Saeed, F.; Vijay, S.; Hojat, K.; Nazanin, F.; Mohammad, E.; Ozgur, K.; Mohammed, A.; Nuruol, M.; Ahmed, E.S. Flood routing in river reaches using a three-parameter muskingum model voupled with an improved bat algorithm. *Water* **2018**, *10*, 1130.
60. Derrac, J.; García, S.; Molina, D.; Herrera, F. A practical tutorial on the use of nonparametric statistical tests as a methodology for comparing evolutionary and swarm intelligence algorithms. *Swarm Evol. Comput.* **2011**, *1*, 3–18. [CrossRef]